J Mater Sci (2009) 44:5939–5943
DOI 10.1007/s10853-009-3818-8

LETTER

Effect of additive composition on microstructure and mechanical properties of SiC ceramics sintered with small amount of RE_2O_3 (RE: Sc, Lu, Y) and AlN

B. V. Manoj Kumar · Myong-Hoon Roh · Young-Wook Kim · Wonjoong Kim · Sang-Whan Park · Won-Seon Seo

Received: 4 May 2009 / Accepted: 18 August 2009 / Published online: 27 August 2009

Silicon carbide is a potential material for various structural applications because of its unique combination of properties such as high hardness, high temperature strength, and excellent resistance to wear and corrosion [1–4]. In order to improve the fracture toughness, several attempts have been made to fabricate SiC ceramics consisting of heterogeneous microstructure with weak grain boundary phases [5–7]. The liquid-phase sintering using metal oxides, Al–B–C, AlN–metal oxides as sintering additives is recommended for obtaining SiC ceramics with tailored microstructure [8, 9]. Among various additive systems, AlN and RE_2O_3 (RE: rare-earth elements) systems are preferred due to relatively less weight loss [10], easy control of oxynitride decomposition, and absence of gas-phase reactions below 2000 °C [6]. The use of RE_2O_3 renders SiC ceramics with excellent high temperature strength and toughness properties [6, 11]. The platelet-reinforced microstructures exhibit enhanced toughness due to combination of intergranular crack mode, introduced by the glassy grain boundary phase, and energy dissipating processes in the crack wake [12]. Though most of the studies reported amorphous grain boundary or ternary junction phase, it has been recently identified that sintering additive composition plays a dominant role in affecting the crystallinity of grain boundary phase. Amorphous intergranular phase was obtained using AlN–Y_2O_3 [13, 14] and AlN–Er_2O_3 [9, 11] additives systems, whereas AlN–Sc_2O_3 render clean grain boundary [15, 16] and AlN–Lu_2O_3 systems render clean [17] or crystallized grain boundary [18]. It is to note that most of the published research has been conducted toward characterization and property evaluation of SiC ceramics prepared with relatively large amounts of additives (≥5 wt%), while its performance with small additive contents is poorly understood. Therefore, an attempt has been made in this study, for the first time, to sinter SiC ceramics using small amount (3 wt%) of AlN–RE_2O_3 (RE: Sc, Lu and Y) additives. The major purpose is to investigate the influence of additive composition on microstructural and mechanical characteristics of SiC ceramics sintered with small additive amounts.

Commercially available β-SiC (Ultrafine grade, Beta-rundum, Ibiden Co. Ltd., Ogaki, Japan), AlN (Grade F, Tokuyama Soda Co., Tokyo, Japan), and metal oxides (Sc_2O_3, Lu_2O_3, and Y_2O_3, 99.9% pure, Shin-Etsu Chemical Co., Tokyo, Japan) were used as the starting powders. The mean particle size and the specific surface area of the β-SiC powders were 0.27 μm and 17.5 m^2/g, respectively. A powder mixture of SiC and 3 wt% additives AlN and RE_2O_3 (RE: Sc, Lu, Y) was prepared. The relative amount of RE_2O_3 in the total content of additives was 20 mol.%. The respective powder batches were milled in ethanol for 24 h using SiC grinding balls. The milled slurry was dried, sieved, and hot-pressed at 2050 °C for 6 h under a pressure of 25 MPa in N_2 atmosphere. The details of specimen designation, batch composition, and additive systems are given in Table 1. The designation SCRE represents silicon carbide specimen prepared using 3 wt% RE–AlN (RE: Sc, Lu, Y) additive.

The bulk density of the sintered specimen was measured using the Archimedes method in water. The theoretical

B. V. Manoj Kumar · M.-H. Roh · Y.-W. Kim (✉) · W. Kim
Department of Materials Science and Engineering,
The University of Seoul, Seoul 130-743, Korea
e-mail: ywkim@uos.ac.kr

S.-W. Park
Materials Science and Technology Research Division,
Korea Institute of Science and Technology, Seoul, Korea

W.-S. Seo
Korea Institute of Ceramic Engineering and Technology,
Seoul 153-801, Korea

Table 1 Details of sintering additive and density of the investigated batch compositions

Specimen designation	Batch composition (wt%)	RE_2O_3/(AlN + RE_2O_3) mol ratio	Density (g/cm^3)	Relative density (%)
SCSC	β-SiC + 1.63 AlN + 1.37 Sc_2O_3	0.2	3.17 ± 0.10	99.2
SCLu	β-SiC + 0.88 AlN + 2.12 Lu_2O_3	0.2	3.20 ± 3.20	94.7
SCY	β-SiC + 1.26 AlN + 1.74 Y_2O_3	0.2	3.09 ± 0.10	98.0

densities of each specimen were calculated according to the rule of mixtures using the following densities: β-SiC 3.216 g/cm^3 (JC-PDF #29-1129), AlN 3.261 g/cm^3 (JC-PDF#25-1133), Sc_2O_3 3.840 g/cm^3 (JC-PDF#43-1028), Lu_2O_3 9.426 g/cm^3 (JC-PDF#43-1021), and Y_2O_3 5.032 g/cm^3 (JC-PDF#43-1036). The sintered specimens were cut, polished in the perpendicular direction to pressing axis, and etched using a CF_4 plasma containing 20% O_2. The grain morphology was observed using scanning electron microscopy (SEM, S4300, Hitachi Ltd., Japan). After regular methods of sample preparation, high resolution transmission electron microscopy (HRTEM, 400 kV, JEM-4010, JEOL, Japan) was used to determine the characteristics of grain boundary phases. For the strength measurements, bar-shaped specimens were ground to a size of 3 mm × 2.5 mm × 25 mm. The tensile surfaces of the bars were polished to 1 μm diamond finish and the tensile edges beveled to avoid stress concentrations and large edge flaws that would cause due to sectioning. Bending tests were performed at room temperature on 4–5 specimens at each condition using a four-point method with an inner and outer span of 10 and 20 mm, respectively. The specimens were loaded at a constant crosshead speed of 0.5 mm/min. The hardness of the polished specimen was measured by the Vickers indentation, done at 2.9 N load for a dwell time of 10 s. The fracture toughness was determined by measuring the crack lengths that were generated by a Vickers indenter with a load of 49 N for a dwell time of 30 s [19].

The influence of additive composition on the density of the sintered SiC specimen is shown in Table 1. The hot pressing of the investigated powder mixtures resulted in a high density (≥98%) for SCSc or SCY, and relatively poor density (~95%) for SCLu specimens. During hot pressing, AlN–RE_2O_3 additives react with the native SiO_2, present on SiC particles to form an Al–RE–Si–oxynitride melt, which upon heating to high temperatures forms Al–RE–Si–oxycarbonitride melt by dissolution of SiC [16–18]. Thus, solution-reprecipitation occurring during liquid-phase sintering (LPS) promotes densification**.** The present results essentially indicate that small amounts (3 wt%) of sintering additives used were sufficient for the densification of Sc_2O_3 and Y_2O_3-containing additive systems. Considering the high viscosity of Lu_2O_3-containing glass phase [20, 21], it was possible that the formation of Lu–Al–Si–oxycarbonitride melt during LPS was not effective for the densification of 3 wt% Lu_2O_3–AlN additive system.

The representative microstructures of the plasma-etched surfaces of the sintered specimens are provided in Fig. 1. The investigated specimens differ in the composition, but contain same amount of total additive content and RE_2O_3/(AlN + RE_2O_3) ratio. The microstructure of SCLu consists of coarse (5–10 μm) equi-axed grains, whereas that of SCY and SCSc showed platelet (elongated, in 2-dimensional) grains (see Fig. 1a–c). XRD analysis of the sintered specimen (Fig. 2) reveals the presence of both β-SiC and α-SiC, indicating $\beta \rightarrow \alpha$ phase transformation occurred during sintering. Also, core-rim morphology observed in the microstructures (see Fig. 1) indicates contribution of solution-reprecipitation mechanism for the grain growth. Thus, the growth of platelet grains resulted from both $\beta \rightarrow \alpha$ phase transformation and solution-reprecipitation. The observed microstructural development is also consistent with the earlier reports [16–18], in spite of small amount of additives used in this study. However, platelet grain

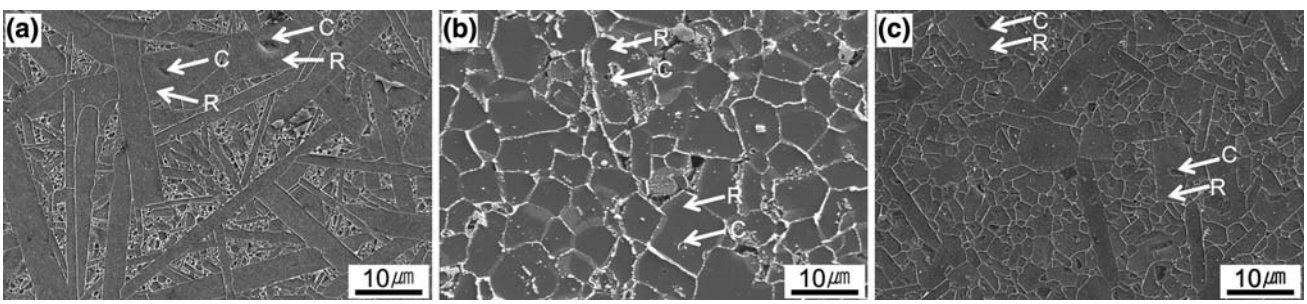

Fig. 1 Typical microstructures of SiC ceramics **a** SCSc, **b** SCLu, and **c** SCY. Core '*C*' and rim '*R*' structure is indicated

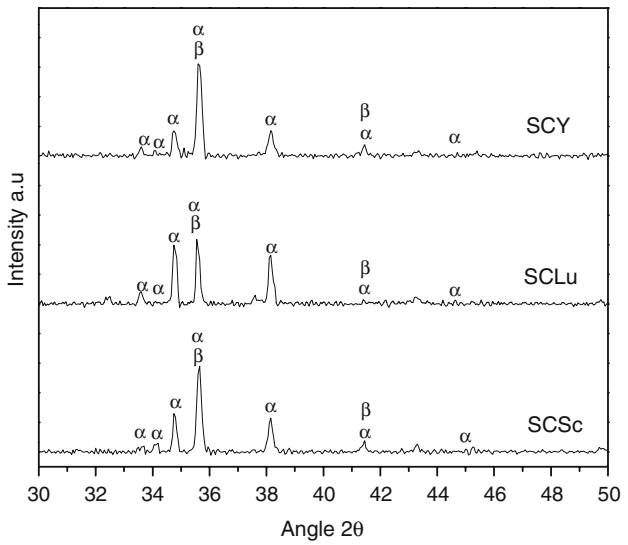

Fig. 2 XRD analysis of the SiC specimens. α and β represent α-SiC and β-SiC phases

morphology was reported when large amount (10 vol.%) of AlN–Lu_2O_3 additives were used. The higher intensity of α-SiC peaks in case of SCLu specimen (Fig. 2) indicates large nucleation of α-SiC responsible for impinging simultaneous abnormal grain growth and thus resulting in a large equi-axed structure of α/β composite grains. It was reported previously that the grain growth occurs initially by Ostwald ripening, followed by growth of composite grains of α-SiC domain sandwiched between β-SiC domains [22]. Further, SCY microstructure consists of large platelet grains and equi-axed grains, while slightly different microstructure of the combination of large, thick platelet grains, and relatively small platelet grains developed for SCSc. The present results suggest that the 3 wt% of AlN–Sc_2O_3 and AlN–Y_2O_3 are efficient additive systems for developing self-reinforced microstructures. Furthermore, it was understood that the cations of additives incorporated into the RE–Al–Si–oxycarbonitride glass phase effectively alter the physical properties, force balance, and, in turn, the thickness of the intergranular film [23]. Typical HRTEM images of the grain boundaries in SCSc and SCY are shown in Fig. 3. Clean grain boundaries without any amorphous phase are observed in SCSc or SCLu specimen, while amorphous phase of ~2.7-nm thickness observed in the grain boundaries of SCY. Therefore, the smaller cation appears to lead the higher tendency for the clean boundaries. These results are consistent with the reported HRTEM studies of systems with 10 vol.% AlN–RE_2O_3 additives [16–18], indicating minimal influence of sintering additive contents on the grain boundary phase characteristics.

Figure 4 shows surface morphology of the fractured specimens of the investigated LPS-SiC ceramics. All specimens exhibit dominant characteristics of transgranular fracture. Usually, crack bridging, frictional grain bridges, elastic bridges are reported as toughening mechanisms for the LPS-SiC ceramics [24, 25]. When crack tip approaches, the platelet grains experience bending stress. As the failure probability for the thin platelet grains is less than that of thick ones, the tendency for crack debonding/bridging would be more in SCY sample when compared with SCSc. Similar observations were reported for SiC ceramics sintered with $Y_3Al_5O_{12}$ and SiO_2 [26] and SiC ceramics sintered with RE_2O_3 (RE: La, Y, Nd, Yb) and Al_2O_3 [27]. Several investigations suggest that the variation in the composition of the sintering additives and hence the composition of the intergranular film can play a significant role in altering the crack propagation behavior of LPS-SiC ceramics [26–28].

The mechanical behavior of SiC ceramics sintered with small amount of additives is represented in terms of hardness, fracture toughness, and flexural strength measurements (Fig. 5). A maximum micro hardness of ~30 GPa is

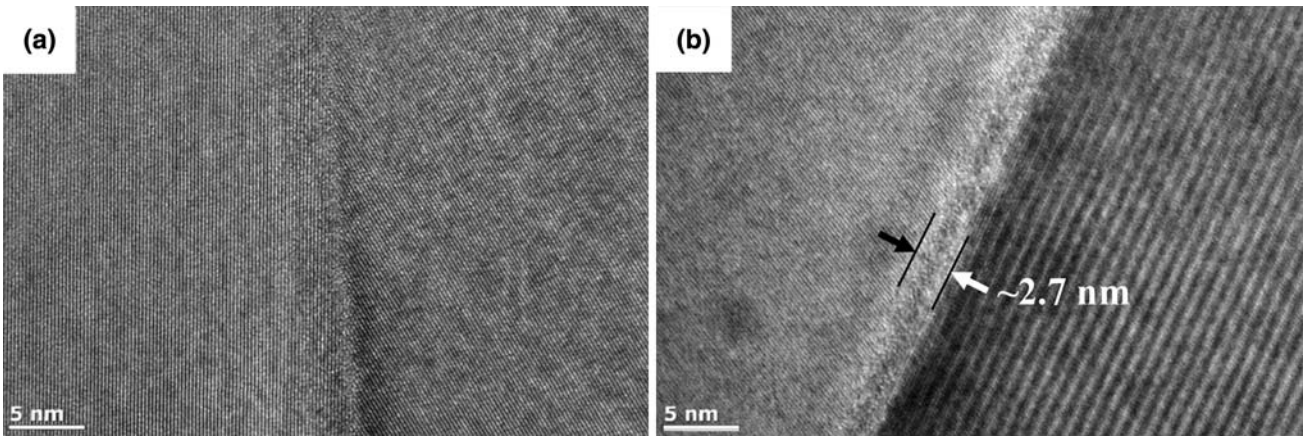

Fig. 3 HRTEM micrographs of SiC ceramics revealing **a** almost clean grain boundary phase in SCSc and **b** amorphous grain boundary phase in SCY

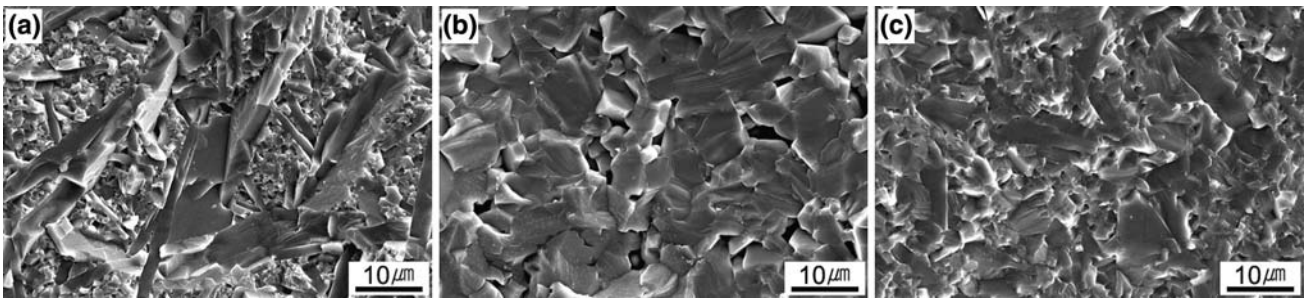

Fig. 4 SEM micrographs of the fracture surfaces of SiC ceramics sintered with 3 wt% AlN and RE_2O_3 (RE: Sc, Lu, Y) additives: **a** SCSc, **b** SCLu, and **c** SCY

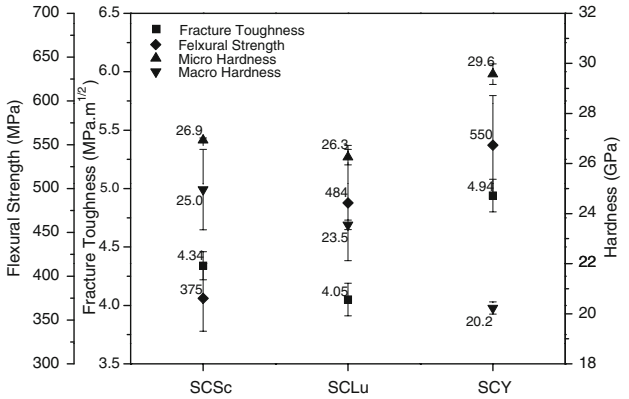

Fig. 5 The variation of mechanical properties of SiC ceramics sintered with 3 wt% of AlN and RE_2O_3 (RE: Sc, Lu, Y) additives

recorded for SCY, while SCLu exhibit minimum micro hardness of 26 GPa. The poor density of the sintered specimen and coarse equi-axed grain structure can be related to the lowest micro hardness measured for SCLu. The bimodal microstructure of platelet grains and equi-axed grains gave the highest micro hardness for SCY, whereas the microstructure of large, thick platelet grains, and small platelet grains resulted in a low micro hardness value for SCSc. In order to estimate the effect of grain boundary phase on the hardness, the hardness measured with high load of 49 N (macro hardness) is also provided in Fig. 5. A maximum reduction of ~9 GPa for SCY specimen corroborates with the amorphous characteristics of the grain boundary phase, whereas a hardness reduction of ~2 GPa in SCSc or SCLu indicates the relatively lower effect of grain boundary phase (Fig. 3). It is evident from Fig. 5 that SCLu specimens possess the lowest fracture toughness of 4.0 MPa $m^{1/2}$, whereas SCY exhibit the highest value of ~5.0 MPa $m^{1/2}$. The measured fracture toughness values of SiC sintered with 3 wt% additives in this study lie in the range of the commonly reported values of 3.5–8.0 MPa $m^{1/2}$ for LPS-SiC ceramics [5, 18, 24, 29]. The low toughness value of SCLu (~4.0 MPa $m^{1/2}$) is attributed to the lack of active toughening mechanisms. The high toughness (~5.0 MPa $m^{1/2}$) of SCY is related to the optimum interfacial strength of platelet grains and equi-axed grains, in the sense that the crack deflection/bridging reduce the tendency for transgranular fracture. The trend in the toughness measurements is in agreement with the HRTEM analysis of the grain boundary phase. The amorphous grain boundary phase along with bimodal microstructure is probably responsible for high fracture toughness for Y_2O_3–AlN additive system, while the absence of amorphous phase in Lu_2O_3–AlN or Sc_2O_3–AlN additive systems exhibits poor toughness. With regards to flexural strength, SCSc exhibit a minimum strength of 375 MPa, while a maximum strength of 550 MPa recorded for SCY. These results are in consistent with the reported flexural strength measurements of 450–650 MPa for the SiC ceramics sintered with different additive compositions [18, 24]. The critical size of the flaws, i.e., pores and grain clusters is significantly less in SCLu (see Fig. 1) might have contributed to the observed high strength [30]. The bimodal platelet and equi-axed grain structure in case of SCY is beneficial in yielding stronger SiC ceramics, while large thick platelet and small platelet grain structure of SCSc resulted in low strength values. The interfacial strength might be optimum for the measured high strength values of SCY specimen.

Comparing the results of this study of small additive systems with the published large additive systems, the following can be realized. With regard to the microstructural development, the smaller amount of additive in Lu_2O_3–AlN systems resulted in a large equi-axed grain structure, whereas all specimens exhibited platelet grain morphology with large amounts of additives (10 vol.%) [17, 18]. The fracture surface morphology is directly related to the microstructural development. With large amount (10 vol.%) of additive systems, dominant characteristics of transgranular fracture were observed for Sc_2O_3–AlN and Lu_2O_3–AlN additives, while mixed mode of intergranular and transgranular fracture noticed for Y_2O_3–AlN additives [15, 18]. In this study, mixed mode of fracture is not observed, but the tendency for the reduced transgranular fracture could be realized with the increased crack debonding/bridging of relatively thin

platelet grains. The hardness measurements at 49 N load in this study are 10–15 GPa less than that measured at 20 N for the large amount of additive systems [31]. Higher fracture toughness of 6.5 MPa $m^{1/2}$ were recorded for the SiC ceramics prepared with 10 vol.% Sc_2O_3 + AlN additives, while low values of 4.3 MPa $m^{1/2}$ were measured in this study [18]. However, the fracture toughness values of 4.0 and 5.0 MPa $m^{1/2}$ recorded for Lu_2O_3–AlN and Y_2O_3–AlN systems in this study are comparable with that measured for the large additive systems (~4.3 and 5.5 MPa $m^{1/2}$). The strength of the ceramics prepared with small additive contents are less than that prepared with large amounts of additives. High strength levels of 620–650 MPa were measured for the SiC ceramics prepared with 10 vol.% additives, whereas the strength varied from 375 to 550 MPa in this study. However, the difference in strength with additive content appeared to vary according to the additive composition. Considering the grain boundary phase analysis of SiC ceramics, crystallization of the intergranular phase causes microcracking and generation of internal stress, which would decrease the flexural strength of the material [29]. The high strength of SCY observed in this study corroborates the observed amorphous grain boundary phase when compared against other systems [18, 23].

In summary, small amount (3 wt%) of Sc_2O_3–AlN or Y_2O_3–AlN systems is sufficient to produce highly densified (>97%) SiC ceramics. The high viscosity of the melt that formed during LPS of Lu_2O_3–AlN additive systems is probably responsible for the poor density (~95%). Among the investigated systems, SCY consisting of bimodal microstructure of large platelet grains and small equi-axed grains with amorphous grain boundary phase is beneficial in yielding hard, tough, and stronger SiC ceramics.

Acknowledgements This work was supported by a grant from the Fundamental R&D Program for Core Technology of Materials, funded by the Ministry of Knowledge Economy, Republic of Korea.

References

1. Lange FF (1975) J Mater Sci 10:314. doi:10.1007/BF00540356
2. Kodera Y, Toyofuku N, Yamasaki H, Ohyanagi M, Munir ZA (2008) J Mater Sci 43:6422. doi:10.1007/s10853-008-2782-z
3. Sciti D, Balbo A, Melandri C, Pezzotti G (2007) J Mater Sci 42:5570. doi:10.1007/s10853-006-0992-9
4. Prabhakaran PV, Sreejith KJ, Swaminathan B, Packirisamy S, Ninan KN (2009) J Mater Sci 44:528. doi:10.1007/s10853-008-3087-y
5. Padture NP (1994) J Am Ceram Soc 77:519
6. Rixecker G, Wiedmann I, Rosinus A, Aldinger F (2001) J Eur Ceram Soc 21:1013
7. Lee SG, Kim YW, Mitomo M (2001) J Am Ceram Soc 84:1347
8. Sigl LS, Kleebe HJ (1993) J Am Ceram Soc 76:773
9. Volz E, Roosen A, Wang SC, Wei WCJ (2004) J Mater Sci 39:4095. doi:10.1023/B:JMSC.0000033388.55299.dc
10. Kim YW, Mitomo M, Nishumura T (2002) J Am Ceram Soc 85:1007
11. Kim YW, Mitomo M, Nishumura T (2001) J Am Ceram Soc 84:2060
12. Becher PF (1991) J Am Ceram Soc 74:255
13. Ye H, Rixecker G, Haug S, Aldinger F (2002) J Eur Ceram Soc 22:2379
14. Biswas K, Schneider J, Rixecker G, Aldinger F (2005) Scripta Mater 53:591
15. Kim YW, Kim SH, Nishumura T, Mitomo M, Lee JH, Kim DY (2005) Key Eng Mater 287:299
16. Kim YW, Lee SH, Nishumura T, Mitomo M (2005) Acta Mater 53:4701
17. Kim YW, Lee JH, Kim DY (2007) Mater Sci Forum 558–559:897
18. Kim YW, Chun YS, Nishumura T, Mitomo M, Lee YH (2007) Acta Mater 55:727
19. Anstis GR, Chantikul P, Lawn BR, Marshall DB (1981) J Am Ceram Soc 64:533
20. Lofaj F, Widerhron SM, Long GG, Hockey BJ, Jemian PR, Browder L, Andreason J, Taffner U (2002) J Eur Ceram Soc 22:2479
21. Ramesh R, Nestor E, Pomeroy MJ, Hampshire S (1997) J Eur Ceram Soc 17:1933
22. Kim YW, Mitomo M, Hirotsuru H (1996) Korean J Cer 2:152
23. Choi HJ, Kim GH, Lee JG, Kim YW (2000) J Am Ceram Soc 83:2821
24. Rixecker G, Biswas K, Rosinus A, Sharma S, Weidmann I, Aldinger F (2002) J Eur Ceram Soc 22:2669
25. Padture NP, Lawn BR (1994) J Am Ceram Soc 77:2518
26. Kim JY, Kim YW, Mitomo M, Zhan GD, Lee JG (1999) J Am Ceram Soc 82:441
27. Zhou Y, Hirao K, Yamauchi Y, Kanzaki S (2002) J Eur Ceram Soc 22:2689
28. Lee SH, Kim YW (2005) J Kor Ceram Soc 42:16
29. Izhevski VA, Bressiani AHA, Bressiani JC (2005) J Am Ceram Soc 88:1115
30. Ko SI, Lee SJ, Roh MH, Kim W, Kim YW (2009) Met Mater Int 15:149
31. Ryu RH, Lee KS, Kim YW (2009) J Mater Sci 44:1416. doi:10.1007/s10853-009-3255-8